The Topographic Effects of Typhoon Nari (2001) during the Landfall Period

Ming-Jen Yang 楊明仁
Institute of Hydrological Sciences, National Central University
Hsiao-Ling Huang 黃小玲
Department of Atmospheric Sciences, National Taiwan University

Abstract

In this study, several 84-h cloud-resolving simulations of Typhoon Nari (2001) are carried out using a quadruply nested-grid mesoscale model MM5 with the finest grid size of 2 km. Analyses of the control simulation show that Nari's eyewall and RMW are upright with a larger eye size and the maximum latent heating is located at the mid- to upper troposphere prior to landfall; after landfall, the reflectivity and RMW axes tilt toward Mt. Snow, with the maximum heating located in the lower troposphere. While the tangential flows are near-axisymmetric, radial flows and latent heating profiles are highly asymmetric. Thus, the damping effects of the friction/terrain-induced radial outflows may be compensated with the intensifying effects of latent heating associated with the torrential rainfall in the maintenance of Nari's constant intensity over Taiwan's island. A series of sensitivity experiments of reducing Taiwan topography are performed to examine the topographic effects on Nari's track, intensity, rainfall distribution and amount. Results show that the impact of island terrain on Nari's intensity is nearly linear, with stronger storm intensity in lower-terrain runs. In contrast, the effects of Taiwan topography on Nari's track and accumulated rainfall amount are nonlinear

1. INTRODUCTION

Typhoon Nari struck Taiwan on September 16, 2001; it brought heavy rainfall, fresh flood, and caused severe economical and societal damage, including 92 human lives (Sui et al. 2002). The first objective of this paper is to investigate whether the model could reproduce the kinematic and precipitation features of the landfalling storm from the given subtropical synoptic conditions, as verified against satellite, rain gague, and radar observations. The second objective is to examine the three-dimensional kinematic and precipitation structures of the storm, with focus on the Central Mountain Range (CMR)-induced structural changes after landfall. The third objective is to examine the topographic effects on the rainfall generation of Nari after landfall. Through a series of terrain sensitivity experiments, we wish to gain insight into the relative importance of the CMR-induced lifting, large-scale flows and Nari's internal dynamics in generating the heavy rainfall over Taiwan.

*Corresponding author address: Dr. Min-Jen Yang, Institute of Hydrological Sciences, National Central University, Chung-Li, Taiwan, 320, ROC. Email: mingjen@cc.ncu.edu.tw

2. METHODOLOGY

The PSU-NCAR MM5 model (Grell et al. 1995) is used to simulate Typhoon Nari (2001). The MM5 model configuration includes four nested grids with horizontal grid size of 54, 18, 6, and 2 km,respectively. The simulation is integrated for 84 h, starting from 120 UTC 15 September 2001. The initial and boundary conditions are taken from the ECMWF advanced global analysis with 1.125° x 1.125° horizontal resolution. The following physics options are used in the control (CTL) simulation: the Grell (1993) cumulus parameterization scheme, the Reisner microphysics scheme with graupel (Reisner et al. 1998), the MRF PBL scheme (Hong and Pan 1996), and the atmospheric radiation scheme of Dudhia (1989). Note that no cumulus parameterization scheme is used on the 6 and 2-km grids. Details in the model setup can be found in Yang et al. (2007).

Based on numerical experiments, Wu et al. (2002) indicated that both the model and terrain resolutions play equal roles in producing heavy rainfall over Taiwan's CMR for Typhoon Herb (1996). To examine to what extent the CMR influences the landfalling characteristics of Nari,

five sensitivity experiments are conducted, in which all model parameters are held the same as those in the CTL simulation except that 75%, 50%, 25%, and 0% of Taiwan terrain elevations are used, respectively, as well as one experiment with ocean conditions over Taiwan. We believe that the impact of replacing the removed mountain volume in these sensitivity simulations is small, because all the model initial flow conditions at levels between 1000 hPa and the layers above, including those in the CTL simulation, are interpolated from the ECMWF/TOGA analyses and used as the first guess field that is then enhanced by the upper-air soundings taken mostly over the plain areas.

3. RESULTS

Figure 1 compares the model-simulated track of Nari to the CWB best-track estimates, using results from the 6-km, larger-area covered domain. In general, the MM5 simulates very well Nari's track, especially its landfall near Yilan at 22 h into the integration (valid at 1000 UTC 16 September, henceforth 16/10), albeit 3 h earlier than and 20 km to the north of the observed. The model also reproduces reasonably well the relatively fast and slow passage of Nari from northeast to southwest across Taiwan before and after 17/00, respectively. However, the simulated track begins to deviate from the observed after 18/12, leading to large displacement errors at the end of the 84-h integration.

It is apparent from Figs. 3 and 4 that the intensity of the simulated Nari responds quite linearly to the changes of Taiwan's topography, but its track responds in a complex manner. Specifically, the lower the Taiwan's terrain height, the deeper central pressure, and the stronger maximum surface wind after landfall. As the terrain heights reduce to zero, Nari's intensity deepens 15 hPa in surface central pressure and increases 6 – 7 m s^{-1} in the maximum surface wind at 17/12 when the simulated storm is fully adjusted to the surface conditions (Figs. 3a,b). The storm intensity of the ocean experiment is slightly stronger than that of no-terrain experiment, owing to the extra contribution of sensible and latent heat fluxes from the underlying ocean surface. The storm intensities of the flat-island and ocean experiments increase after 18/00 when the simulated storms are displaced into the Taiwan Strait (Fig. 4d).

On the other hand, reducing Taiwan's terrain height causes quite irregular changes to the storm track (Fig. 4). That is, with the reduced topography, the simulated storms with stronger intensities tend to move faster than the CTL storm as approaching northern Taiwan under the influence of the easterly steering flows, and track more along the east coast immediately after landfall. Of interest is that during their southwestward journeys the storms turn around to form a circle between 16/18 and 17/18, with smaller radii for lower terrain heights (cf. Figs. 2 and 4a,b,c). When the topography is completely removed, the simulated storm only dips southwestward on the first day, but turns (after a small "circle") northwestward on the second day, and then southwestward afterwards by the environmental steering flows (Figs. 2 and 4d). The simulated track of the ocean experiment follows closely to that of the no-terrain experiment (not shown). Based on the sensitivity simulations, it appears that Taiwan's topography tends to slow down Nari's southwestward movement, and the high CMR ridge helps keep Nari's track on its west side after passing its peak from the east. Thus, we may state that Nari's track after landfall results from the complex interactions between the environmental steering flow, Taiwan's topography, and the terrain-induced mesoscale forcings; realistic terrain information should be prescribed in order to provide more accurate track prediction of TCs, at least for the case of Nari.

In view of the marked directional changes and displacement in the simulated tracks after landfall, it is meaningful to compare only the first 24-h accumulated rainfall from the 6-km grid for these sensitivity simulations (Table 1). It is important to note that while higher terrain causes the storm to weaken at a faster rate, it tends to enhance rainfall on the windward side of the CMR, thus increasing the total accumulated amount. That is, the higher terrain heights used, the more is the total accumulated rainfall (see Table 1). The slightly more rainfall in the 75% terrain run than that in the CTL appears to be caused by the more residence time of the storm over the island. However, this enhancement effect is not all linear for local rainfall maxima. This result may be related to the nonlinear interaction of topography with the storm's internal dynamics. With more evaporation from the underlying ocean surface, the ocean experiment produces slightly more rainfall than the no-terrain experiment (Table 1 and Fig.4d), as expected. The area-averaged 24-h accumulated rainfall amounts within three different radii from Nari's centers are given in Table 2, which shows again an expected general trend of decreasing "storm-scale" rainfall with reducing terrain heights over Taiwan.

ACKNOWLEDGEMENTS

This research is supported by the National Science Council in Taiwan, ROC, under Grants NSC 95-2111-M-008-005-AP1. The authors thank Prof. Da-Lin Zhang for his suggestions on the control and terrain sensitivity experiments.

REFERENCES

Dudhia, J. 1989: Numerical simulation of convection observed during the Winter Monsoon Experiment using a mesoscale two-dimensional model. *J. Atmos. Sci.*, **46**, 3077-3107.

Grell, G. A., 1993: Prognostic evaluation of assumptions used by cumulus parameterizations. *Mon. Wea. Rev.*, **121**, 764-787.

Grell, G. A., J. Dudhia, and D.R.Stauffer,1995: A description of the fifth-generation Penn State/NCAR Mesoscale Model. NCAR Technical Note,122 pp.

Hong, S.-Y., and H.-L. Pan, 1996: Nocturnal boundary layer vertical diffusion in a medium-range forecast model. Mon. Wea. Rev., 124, 2322-2339.

Reisner, J., R. J. Rasmussen, and R. T. Bruitjes, 1998: Explicit forecasting of supercooled liquid water in winter storms using the MM5 mesoscaled model. *Quart. J. Roy. Meteor. Soc.*, **124**, 1071-1107.

Sui, C.-H., and Coauthors, 2002: Meteorology-hydrology study targets Typhoon Nari and Taipei flood.. *Eos*, Transctions, AGU, **83**, 265, 268-270.

Wu, C.-C., T.-H. Yen, Y.-H. Kuo, and W. Wang, 2002: Rainfall simulation associated with Typhoon Herb (1996) near Taiwan. Part I: The topographic effect. *Wea. Forecasting*, **17**, 1001-1015.

Yang, M.-J., H.-L. Huang, and D.-L. Zhang, 2007: A modeling study of Typhoon Nari (2001) at landfall. Part I: The topographic effects. *J. Atmos. Sci.*, revised.

Table 1: The percentage of the island-averaged 24-h accumulated rainfall on 16 September 2001 from each 6-km sensitivity experiment with respect to the control simulation.

Variable	CTL	75%Ter	50%Ter	25%Ter	0%Ter	Ocean
Percentage wrt. CTL (%)	100.0	102.9	88.2	70.0	51.9	52.3

Table 2: The percentage of the area-averaged 24-h accumulated rainfall within 100-km, 150-km, and 200-km radii from the typhoon center on 16 September 2001 from each 6-km sensitivity experiment with respect to the control simulation.

Radius	Number of points	CTL	75%Ter	50%Ter	25%Ter	0%Ter	Ocean
100 km	877	100	97.3	84.2	64.7	62.2	61.5
150 km	1961	100	94.1	85.1	68.5	64.9	64.1
200 km	3503	100	95.4	84.0	71.8	66.3	68.3

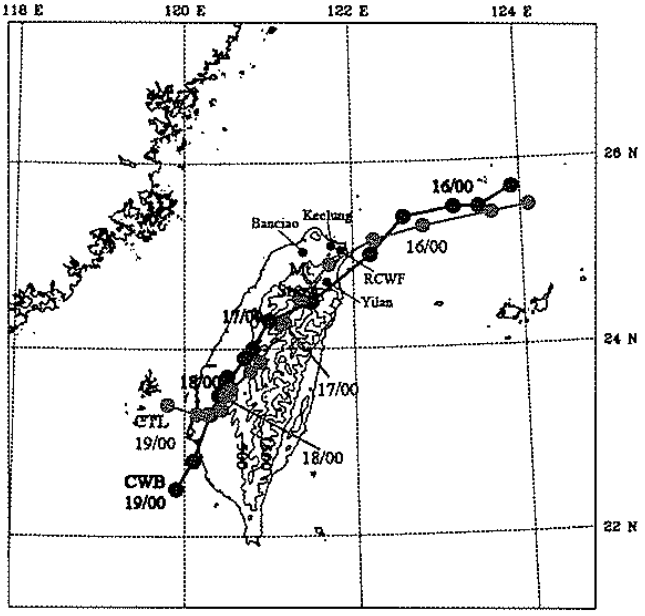

Figure 1: Comparison of the CWB best track (CWB; thick solid) and the simulated track (CTL; grey solid) of Typhoon Nari, superposed with the terrain height (thin solid) at 1000-m intervals (starting at 500-m height). Each dot denotes Nari's central position every 6 h. The inset table is for the simulated track error with respect to the CWB analysis at 12 hourly intervals.

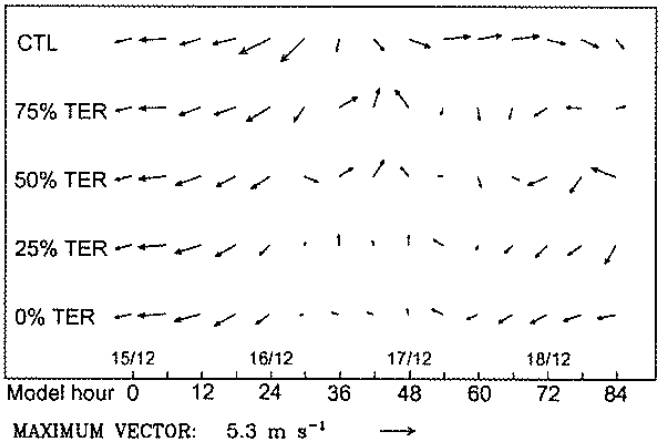

Figure 2: Environmental steering flow vectors from the control and terrain sensitivity experiments that are calculated by averaging horizontally within a radius of 200 km from the simulated Nari and vertically between 900 and 100 hPa.

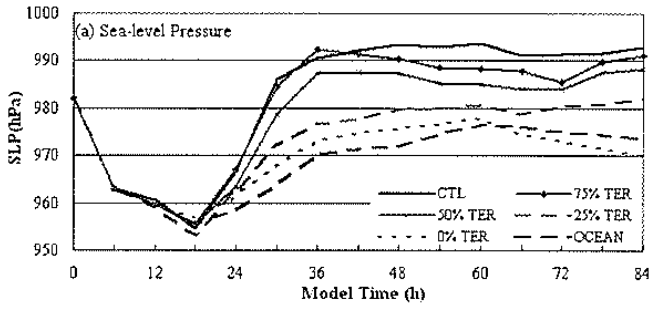

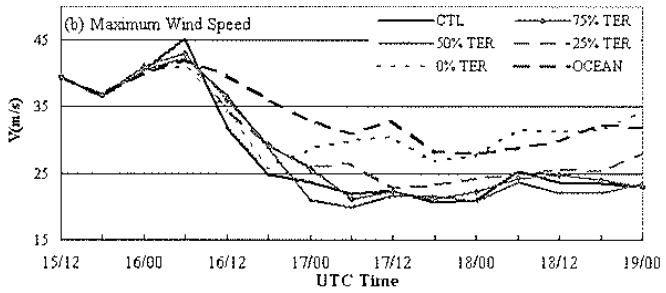

Figure 3: Time series of (a) the minimum sea level pressure (SLP; in units of hPa) and (b) the surface maximum wind (V; in units of m s^{-1}) for the sensitivity simulations to reduced terrain heights using 75%, 50%, 25%, and 0% of the terrain height field and ocean condition (OCEAN) in the control run. The 6-km control simulation (CTL) is also shown.

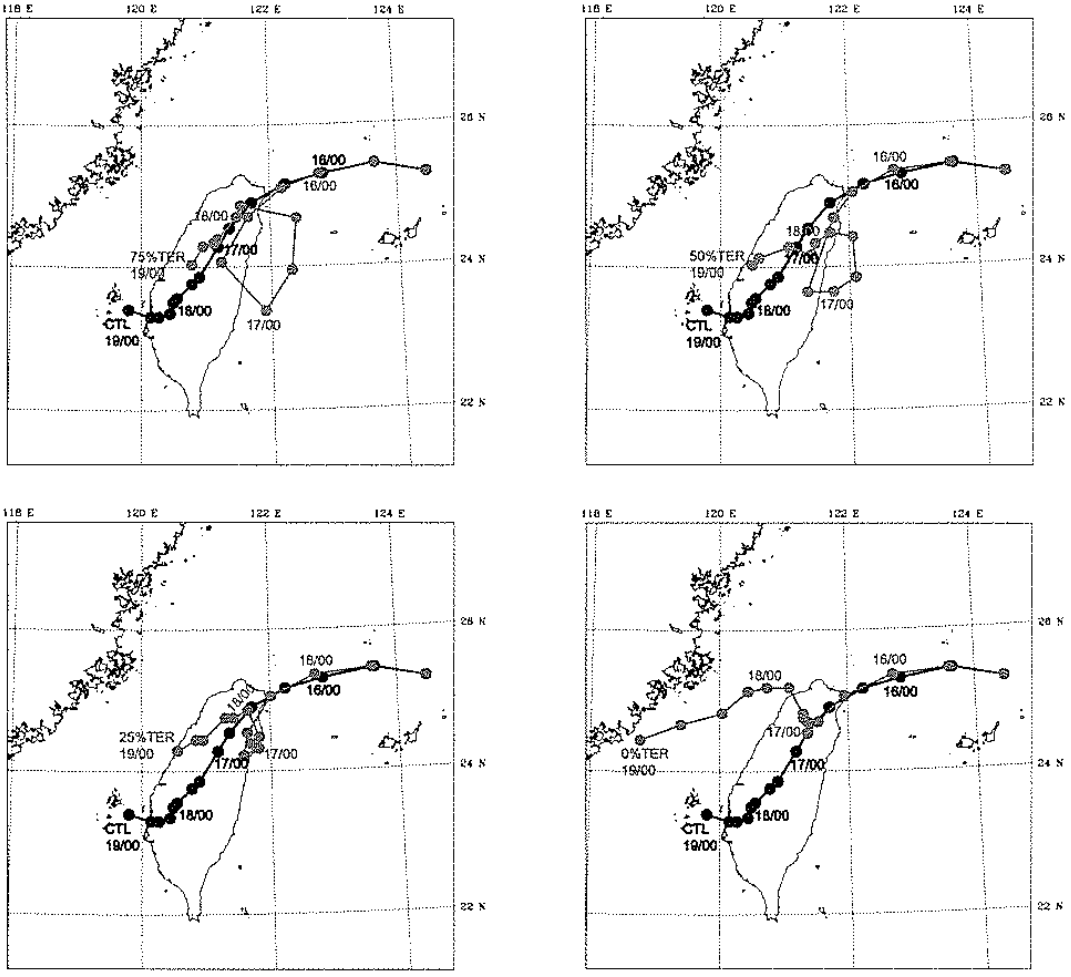

Figure 4: As in Fig. 1 bur for the terrain sensitivity experiments using (a) 75%, (b) 50%, (c) 25%, and (d) 0% of the terrain height field in the control run. The control-simulated track (CTL) is also shown.